



# Mechanical properties of SiC nanoparticle-reinforced Al-2024 alloy

M. B. Niyaz Ahamed\*

*Engineering Department, College of Engineering and Technology, University of Technology and Applied Science, Shinas, Sultanate of Oman.*

*Niyaz.budensab@utas.edu.om*

H. S. Naveen Kumar

*Department of Mechanical Engineering, Government Polytechnic, Holenarasipura, Karnataka, India.*

*naveen.2416932@ka.gov.in; <http://orcid.org/0000-0001-8203-3460>*

S. Kallimani Anilkumar

*Department of Mechanical Engineering, Government Engineering College, Huvinabadagali, VijayaNagar, Karnataka, India.*

*anilskallimani@gmail.com; <http://orcid.org/0009-0006-4477-4122>*

Alqahtani Ibrahim

*School of Aerospace, Transport and Manufacturing, Cranfield University, College Road, Cranfield MK43 0AL, UK*

*I.alqahtani@cranfield.ac.uk*

Doddamani Saleemsab

*Department of Mechanical Engineering, National Institute of Technology Karnataka, Surathkal, Karnataka, India.*

*saleemsabdoddamani@gmail.com; <http://orcid.org/0000-0002-8498-1488>*

G. Hareesha

*Department of Mechanical Engineering, Government Engineering College, Gangavathi, Karnataka, India.*

*barishsb@gmail.com; <http://orcid.org/0000-0003-1274-9716>*



**Citation:** Niyaz Ahamed, M. B., Naveen Kumar, H. S., Kallimani, S. A., Alqahtani, I., Doddamani, S., Hareesha, G., Mechanical properties of SiC nanoparticle-reinforced Al-2024 alloy, *Frattura ed Integrità Strutturale*, 72 (2025) 148-161.

**Received:** 02.02.2025  
**Accepted:** 17.02.2025  
**Published:** 20.02.2025  
**Issue:** 04.2025

**Copyright:** © 2025 This is an open access article under the terms of the CC-BY 4.0, which permits unrestricted use, distribution, and reproduction in any medium, provided the original author and source are credited.



**KEYWORDS.** Al2024 Alloy, Silicon carbide nanoparticles, hardness, tensile strength, fractography, Strengthening Mechanism.

## INTRODUCTION

Aluminum alloys, especially Al-2024, are widely utilised in high-performance industries like the automotive, marine, and aerospace sectors because of their good fatigue, corrosion resistance, and the strength-to-weight ratio [1]. Al-2024, like many other aluminium alloys, has limitations regarding mechanical performance, hardness, and wear resistance under harsh operating circumstances [2]. Overcoming these obstacles and strengthening Al-2024 with ceramic particles has become a viable strategy for improving its mechanical characteristics [3].

Microparticles have been utilised to strengthen metal matrix composites because they improve characteristics, including strength, wear resistance and hardness [4]. Alternatively, nanoparticles' large surface area-to-volume ratio allows for significant particle-matrix interaction and yields noticeably superior results [5]. Nanoparticles provide better mechanical strengthening than micro-sized particles because of their finer dispersion within the matrix, which enhances load transfer, decreases agglomeration, and improves control over the spread of cracks [6]. Additionally, nano-sized reinforcements aid in the refinement of the grain structure, enhancing mechanical properties such as fatigue resistance, hardness, and tensile strength [7]. Even though microparticles can improve mechanical properties, their usefulness is limited because they commonly produce clustering and uneven distribution within the matrix [8,9]. However, when appropriate methods were applied to integrate nanoparticles into the matrix, they provided a more consistent dispersion.

Achieving a uniform distribution of reinforcement depends majorly on the particle inclusion technique. Conventional stir casting is a widely used method for creating metal matrix composites, because of its ease of use and affordability [10–13]. Stir casting procedure uses mechanical stirrer to mix micro or nano-reinforcing particles into the molten metal. However, poor particle distribution of nanoparticles into matrix material limits the use stir casting [5]. The efficiency of nanoparticles in enhancing mechanical properties may be reduced by clustering, agglomeration, and inadequate wettability between the reinforcing particles and the matrix. Because of their high surface energy, these difficulties become more noticeable with smaller particle sizes, such as nanoparticles.

The alternative method has been developed to overcome these limitations such as ultrasonic-assisted stir casting which is emerged as the cutting-edge technology to prepared the metal matrix composites (MMC). In the process of stirring, this technique induces ultrasonic vibrations in the molten metal [14]. The cavitation effects produced by the ultrasonic vibrations disintegrate clusters of nanoparticles and enhance the wettability of reinforcement with the aluminium matrix [15]. Thus, it leads to a better particle-matrix contact and a more uniform distribution of nanoparticles. Achieving these is essential for attaining significant mechanical properties [16]. In addition to facilitating de-clustering of nanoparticle, the ultrasonic cavitation process ensures the particles are uniformly distributed throughout the matrix [17]. Ultrasonic-assisted stir casting method works well when adding nano-sized reinforcements, such as silicon carbide (SiC), where uniform distribution is critical in achieving the reinforcement's full potential.

Integration of SiC nanoparticles into the Al-2024 alloy matrix is a viable approach in addressing the material's critical obstacles. This is particularly effective in enhancing hardness and overall mechanical performance under demanding circumstances. Even though knowing the benefits of using nanoparticle reinforcements over microparticles, it is still challenging to distribute these particles uniformly throughout the metal matrix. The novelty of this study includes employing ultrasonic-assisted stir casting to achieve uniform dispersion of SiC nanoparticles in Al-2024 alloy, enhancing hardness and tensile strength for advanced engineering applications. In order to maximize the mechanical properties of the composite material, this work used ultrasonic-assisted stir casting to ensure the homogeneous distribution of SiC nanoparticles. The relationship between particle distribution, hardness and tensile strength in Al-2024 alloys will be studied experimentally with varying SiC nanoparticles. This work will offer a primary understanding of the potential of nanoparticle-reinforced composites for advanced engineering applications.

## MATERIALS AND METHODS

### *Materials*

Al-2024 is a high-strength aluminium alloy widely used in structural, automotive, and aerospace applications because of its excellent fatigue resistance, machinability, and strength-to-weight ratio. The main alloying element in Al-2024 alloy is copper, which increases its strength, while other components like silicon, magnesium, and manganese help



improve the mechanical properties. The chemical composition and mechanical properties of Al-2024 alloy is given in Tab. 1.

Element	Composition
Cu (%)	4.1
Mg (%)	1.6
Mn (%)	0.7
Si (%)	0.07
Zn (%)	0.03
Fe (%)	0.2
Property	Value
Density (g/cm <sup>3</sup> )	2.78
Ultimate tensile strength (MPa)	175
Yield strength (MPa)	125
Elongation at break (%)	12-14

Table 1: The chemical composition and mechanical properties of Al-2024 alloy [2].

Al-2024 has significant mechanical qualities, but its wearability and decreased hardness limit its applicability in high-abrasion and critical operating environments. As a result, adding ceramic reinforcements, like silicon carbide (SiC) nanoparticles, can improve the alloy's hardness and resistance to deformation and wear.

The reinforcing material for this study was silicon carbide (SiC), which was selected due to its remarkable mechanical properties, such as its high hardness and temperature endurance, and its compatibility with aluminium matrices. The density of SiC nanoparticles, which is nearly identical to that of Al-2024 alloy (2.78 g/cm<sup>3</sup>), is one of the main reasons for selecting them. During the casting process, SiC's density (about 3.21 g/cm<sup>3</sup>) is close enough to Al-2024 to improve particle dispersion inside the matrix [18]. Because of their similar densities, the SiC particles in the molten aluminium settle less, resulting in a more even dispersion across the matrix. The following are essential characteristics of SiC nanoparticles: melting point: 2730°C, thermal conductivity: 120 W/mK, hardness: 9.5 on the Mohs scale, and Young's modulus: 450 GPa [17].

SiC works well with aluminium alloys because it improves load-bearing capacity, decreases dislocation motion, and refines grain structure, reinforcing the matrix. Better particle-matrix interaction and consistent stress distribution are made possible by SiC nanoparticles' larger surface area-to-volume ratio than microparticles. As a result, mechanical qualities, including hardness, tensile strength, and wear resistance, significantly improve. These improvements are essential for prolonging the useful life of Al-2024 alloy components.

In this study, the SiC nanoparticles were added to the Al-2024 matrix in different weight fractions (1%, 2%, 3%, and 4%) using the ultrasonic-assisted stir-casting technique. This technique was selected to maximise the composite's mechanical benefits by achieving homogeneous dispersion of the SiC nanoparticles within the matrix.

### *Casting*

SiC nanoparticles (1%, 2%, 3%, and 4% by weight) were preheated to 250°C to remove moisture and contaminants and to match the temperature of the molten Al-2024, improving wettability and bonding with the matrix.

As seen in Fig. 1, the Al-2024 alloy was melted in a graphite crucible at 750°C in an electric resistance furnace [19]. A cover flux was used to guarantee a clean, homogenous melt and prevent oxidation. The molten alloy was mechanically stirred at 300 to 400 rpm for five to ten minutes while hot SiC nanoparticles were added. To ensure uniform dispersion throughout the matrix and break up clusters of nanoparticles, ultrasonic cavitation was delivered for five minutes using a 20 kHz ultrasonic probe. The distribution of nanoparticles and particle-matrix bonding were enhanced by the combination of mechanical churning and ultrasonic cavitation [4].

The impact of different SiC nanoparticle contents on the microstructure and mechanical properties was assessed by metallographic analysis and mechanical testing of the cast composites. Hardness and tensile strength tests were conducted on polished and etched samples for microstructural characterisation in order to evaluate the performance improvements caused by the SiC reinforcement.

### *Specimen Preparation*

After casting, the Al-2024/SiC composite was sectioned into cylindrical specimens as shown in Fig. 2(a). These were polished to a smooth, defect-free surface following ASTM E10 standards to ensure accurate Brinell hardness testing [20]. Polishing involves grinding and finishing to achieve a mirror-like surface. Tensile specimens (Fig. 2(b)) were machined from the cast composite following ASTM E8 standards. Dog-bone-shaped specimens were prepared, with the gauge section

carefully machined and polished to remove any surface defects. After that, these specimens were prepared for tensile testing, which assessed mechanical properties like elongation and tensile strength.

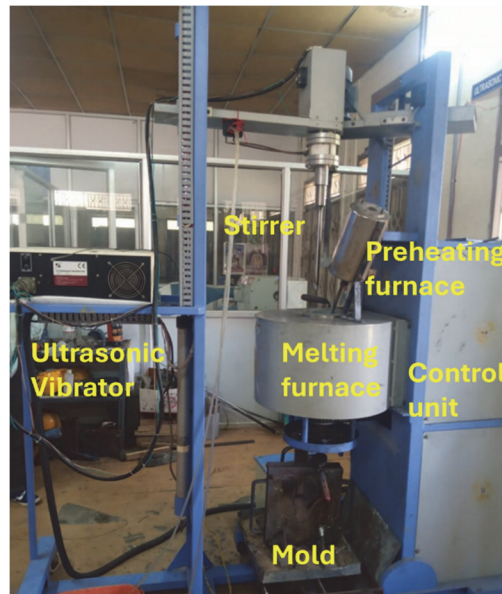


Figure 1: Ultrasonic Stir casting setup.

### Testing

Three samples of each composition (1%, 2%, 3%, and 4% SiC) underwent the Brinell hardness test following ASTM E10. Indentations were made using a steel ball indenter, and the size of the indentation and the applied load were used to determine the Brinell hardness number (BHN). Each composition's average hardness value was noted.

For every composition, tensile tests were performed on three dog-bone-shaped specimens. Three readings were obtained for every specimen, for both tensile and hardness test to ensure consistency. A universal testing machine (UTM) was used to provide axial tensile force to the specimens. Analysis was done using the average tensile strength values, yield strength, and % elongation values.

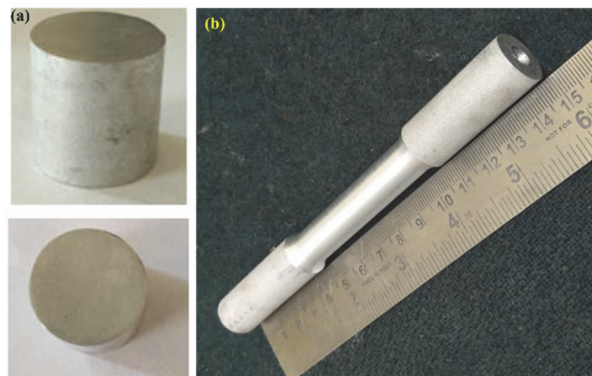


Figure 2: Specimens (a) Hardness, (b) Tensile.

## RESULTS AND DISCUSSIONS

### Microstructure

The Al-2024 alloy's energy dispersive spectroscopy (EDS) mapping is shown in Fig. 3(a), which also shows the distribution of the alloy's component elements: silicon (Si), copper (Cu), magnesium (Mg), manganese (Mn), oxygen (O), and aluminium (Al). As the main structural element, the mapping shows that aluminium is uniformly distributed throughout the alloy matrix. It is apparent in particular areas because copper contributes to the alloy's strength and fatigue

resistance. Additionally dispersed throughout the matrix are magnesium and manganese, each of which gives the alloy special qualities including increased mechanical performance and resistance to corrosion.

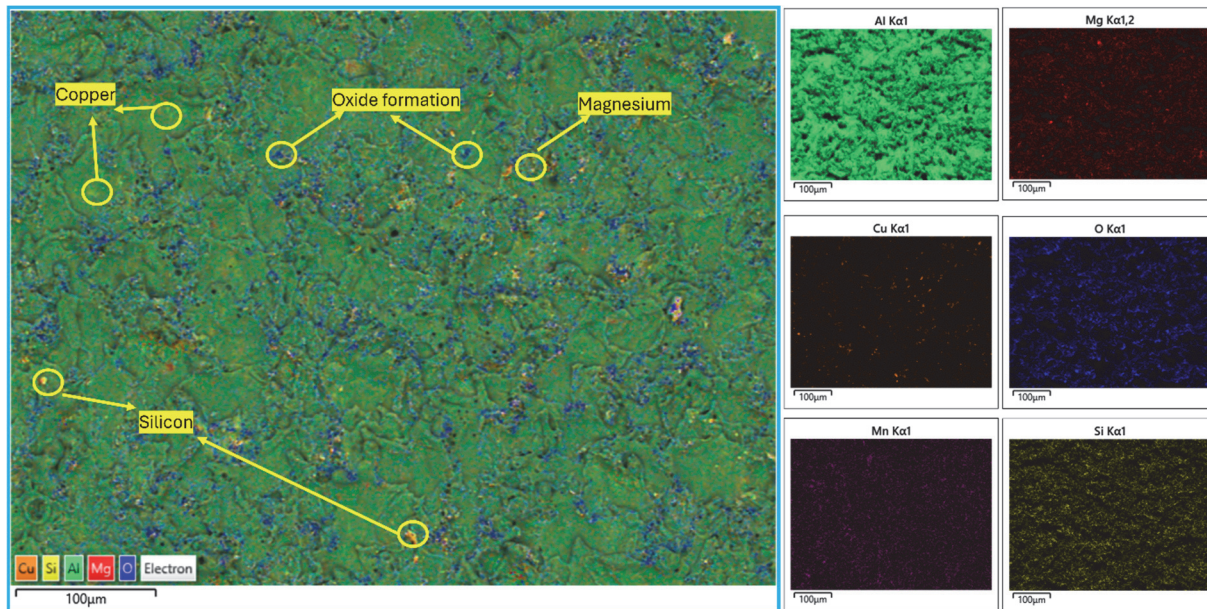


Figure 3(a): EDS mapping of Al-2024 alloy.

A common occurrence with aluminium alloys is oxygen, which may indicate minor surface oxidation, while the sporadic detection of silicon could be due to trace amounts in the alloy or surface impurities. This EDS mapping provides information on the Al-2024 alloy's homogeneity and microstructural properties while validating its elemental makeup.

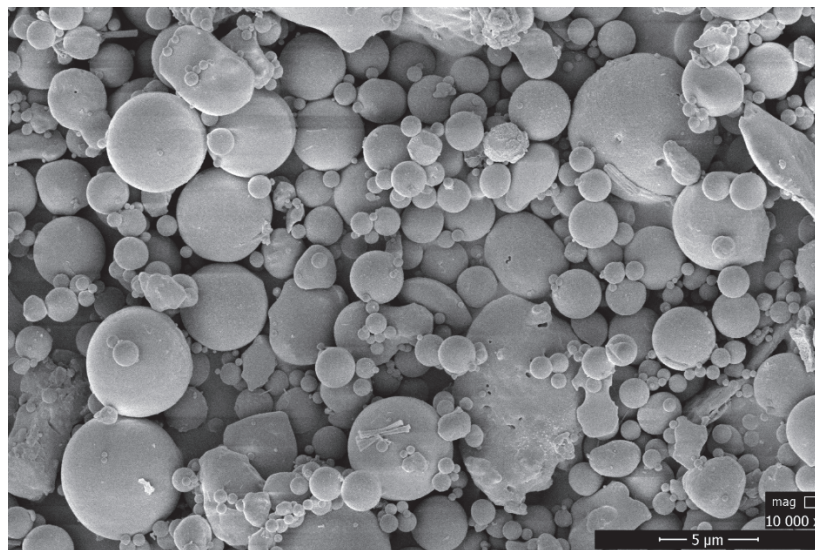


Figure 3(b): Nano-particles of SiC.

An SEM picture of SiC nanopowder is seen in Fig. 3(b), demonstrating the spherical shape of the particles. It is beneficial to have a homogeneous distribution inside composite materials since the particles appear to be uniform in size and shape. By minimising surface area, the spherical shape improves dispersion within the Al-2024 alloy matrix and lessens agglomeration tendencies. This morphology makes continuous bonding contact with the matrix possible, which also improves the mechanical properties of the composite. By offering several locations for load transfer, the size and homogeneity of these nanoparticles also facilitate efficient reinforcing, which enhances the alloy's strength and hardness. Important information on the elemental composition and distribution is revealed by the EDS analysis of Al2024 composites with different SiC (Silicon Carbide) weight percentages—1 wt%, 2 wt%, 3 wt%, and 4 wt%—as illustrated in Fig. 4. The



spectrum shows mostly copper and aluminium at 1 weight percent, with very little SiC. The EDS data show a greater presence of silicon and carbon as the SiC level rises to 2 weight percent, indicating better interfacial bonding and preliminary improvements in mechanical characteristics. The Si and C peaks noticeably increase at 3 weight percent, which is consistent with improved hardness and tensile strength brought on by improved load transfer mechanisms. Finally, at 4 wt%, the EDS analysis shows the highest peaks for Si and C, indicating substantial SiC incorporation, which may lead to significant improvements in mechanical performance. However, potential agglomeration could be a concern.

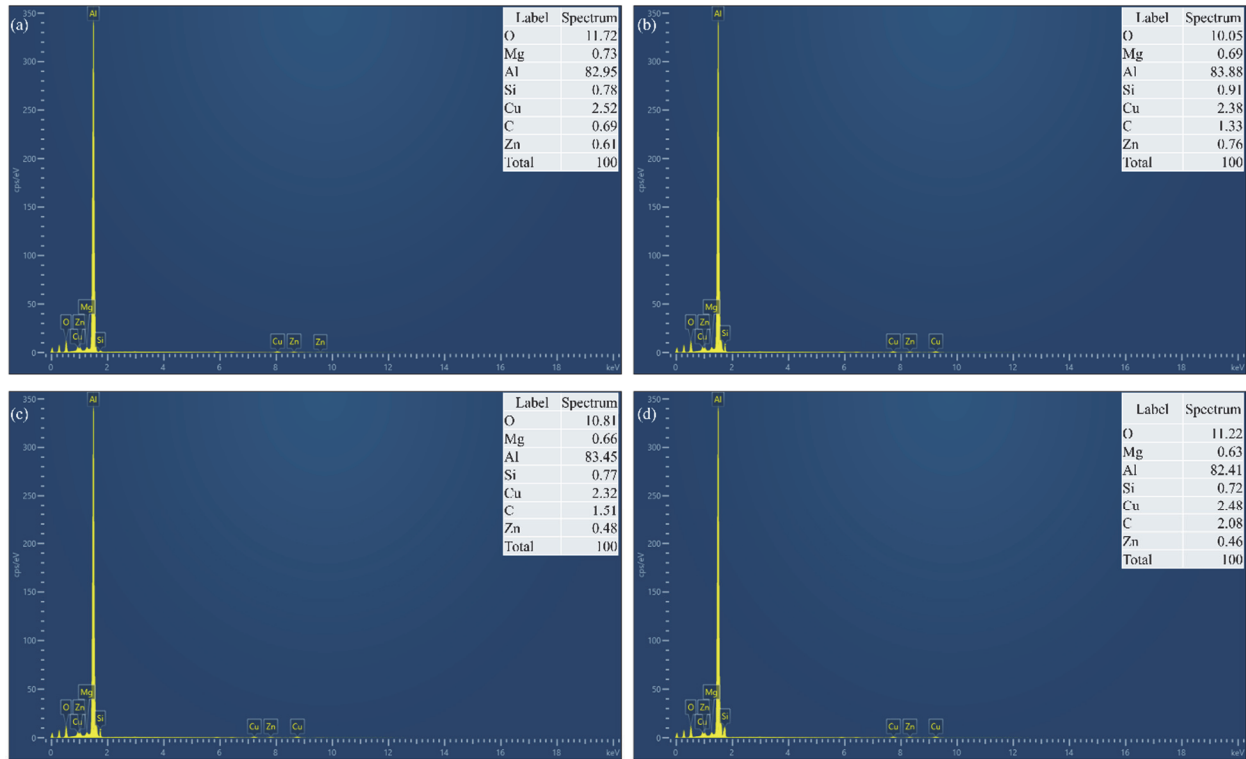


Figure 4: EDS composition of the Al2024 composites with (a) 1wt%, (b) 2wt%, (c) 3wt%, (d) 4wt% of SiC

Fig. 5 displays the Al-2024-SiC nanoparticle composites' X-ray diffraction (XRD) patterns for various SiC weight fractions (0%, 1%, 2%, 3%, and 4%). Utilizing Cu-K $\alpha$  radiation ( $\lambda = 1.5406 \text{ \AA}$ ) at 40 kV and 30 mA of current, the analysis was carried out. With a step size of  $0.02^\circ$  and a counting time of one second per step, the scans spanned a  $2\theta$  range of  $30^\circ$  to  $90^\circ$ . The crystalline phases of the SiC reinforcement and the Al-2024 alloy matrix are represented by distinct diffraction peaks in the XRD patterns. The intensity of the SiC-related peaks intensifies as the SiC weight fraction rises from 1% to 4%, suggesting a steady rise in the matrix's SiC nanoparticle concentration. Together with other peaks that correspond to SiC reinforcement, the notable aluminum peaks are seen at distinctive  $2\theta$  values, confirming the effective integration and even dispersion of SiC nanoparticles in the Al-2024 matrix.

Interestingly, no extra peaks that would indicate secondary phases or intermetallic compounds are seen, suggesting that the SiC particles stay evenly distributed throughout the ultrasonic-assisted stir-casting process without experiencing any unintended reactions. This implies that the procedure successfully creates a uniform composite while maintaining the stability of the SiC reinforcement and the Al-2024 matrix. The peaks' clarity and intensity attest to the reinforced material's structural stability and crystallinity. The observed mechanical increases in the composite are supported by the distinct separation of diffraction peaks, which guarantees that the reinforcement stays in its intended phase.

The distribution of SiC nanoparticles in Al-2024 alloy was assessed microscopically in samples of prepared composites with dimensions of  $10\text{mm} \times 10\text{mm} \times 10\text{mm}$ . The microstructures of the as-cast composite samples with 1, 2, 3, and 4 wt% SiC nanoparticles treated by ultrasonic vibrations aided the stir casting process are shown in Fig. 6(a-d). The micrographs demonstrate how adding nano-sized SiC particles and ultrasonic treatment refined the matrix grains. Using a high-resolution scanning electron microscope (SEM), additional research was done on the generated composite samples to examine the homogeneity of the reinforcement particle distribution in the matrix alloy. According to the SEM micrographs, very few microclusters are still visible in the alloy's matrix, with well-distributed nanoparticles. This demonstrates that high-intensity

ultrasonic vibrations can create intense cavitation, breaking agglomerations apart and dispersing particles with a powerful explosive effect.

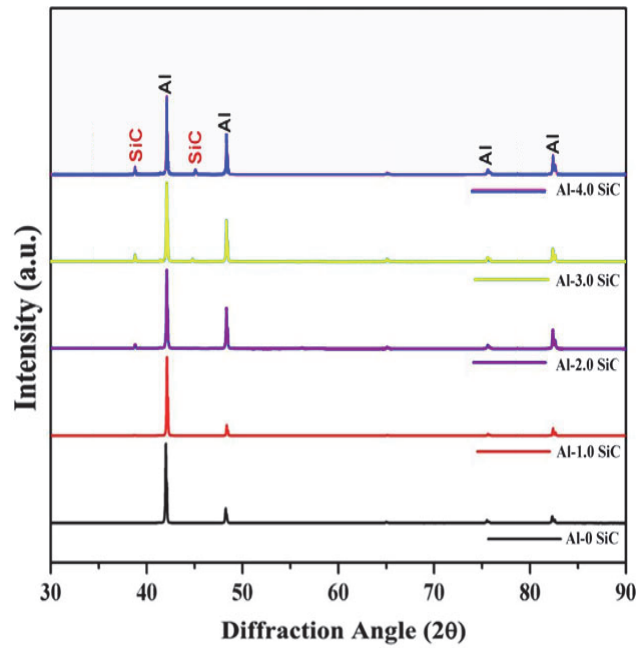


Figure 5: XRD plot for different compositions of Al<sub>2024</sub>-SiC composites.

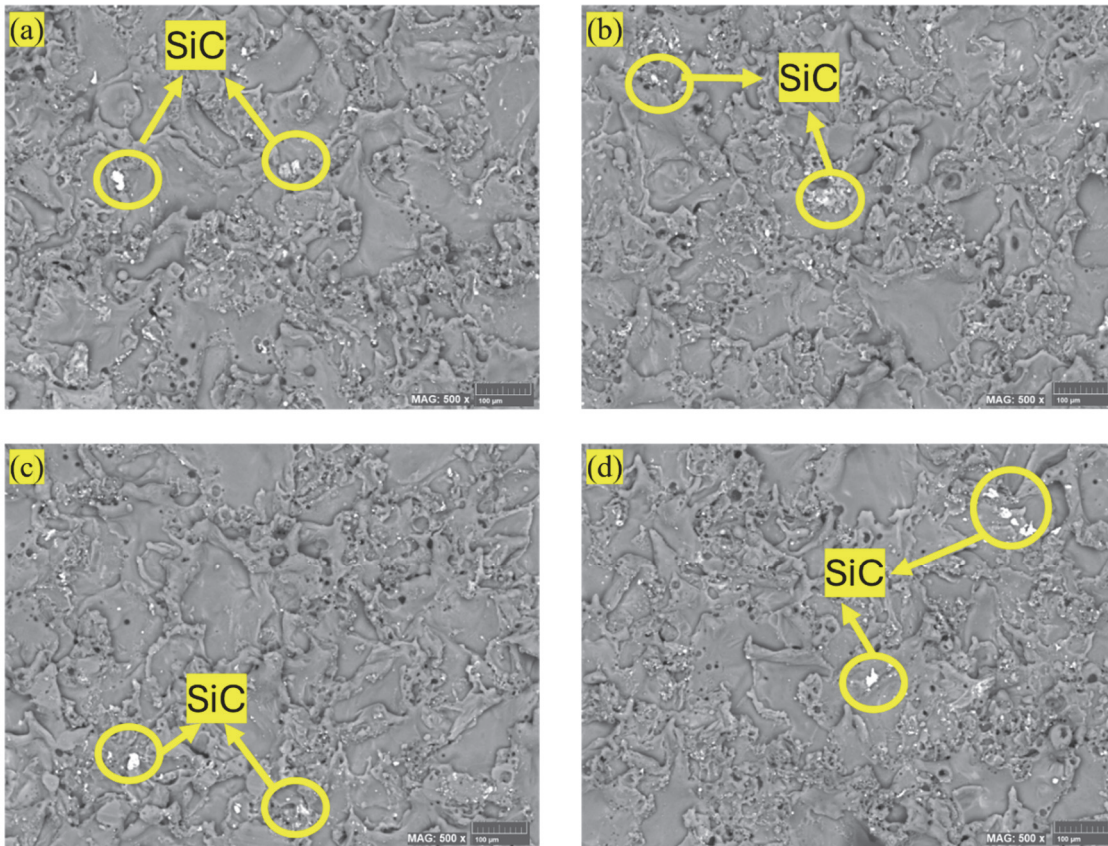


Figure 6: Micrographs show the grain refinement for SiC dispersion in the Al<sub>2024</sub> composites: (a) 1wt%, (b) 2wt%, (c) 3wt%, (d) 4wt% of SiC.



### Hardness

The hardness (BHN) results, shown in Fig. 7, demonstrate a clear trend in the mechanical enhancement of the Al-2024 alloy with the incremental addition of SiC nanoparticles. The pure Al-2024 alloy exhibits a baseline hardness of 90.2 BHN. Adding 1% SiC increases the hardness to 117.0 BHN, while 2% SiC further improves it to 131.2 BHN, indicating effective particle dispersion and enhanced load transfer within the matrix. At 3% SiC, the hardness slightly rises to 132.3 BHN, suggesting a possible saturation in reinforcement benefits. However, with 4% SiC, the hardness drops to 120.0 BHN. This decrease can be attributed to nanoparticle agglomeration, which disrupts uniform particle distribution and weakens interfacial bonding, leading to stress concentration sites and reduced strengthening efficiency.

The results suggest that the optimal reinforcement range for improved hardness in Al-2024 with SiC nanoparticles is 2–3% by weight. The hardness testing revealed a notable 31% enhancement in hardness values with the addition of SiC nanoparticles, demonstrating the effectiveness of nanoparticle reinforcement in improving material properties.

The increase in hardness values of the Al-2024-SiC composite is primarily due to the uniform distribution of nano-sized particles, which effectively limit dislocation movement. The SiC particles act as load-bearing reinforcements, improving load transfer and resistance to indentation. Additionally, the presence of SiC promotes grain refinement, further enhancing hardness..

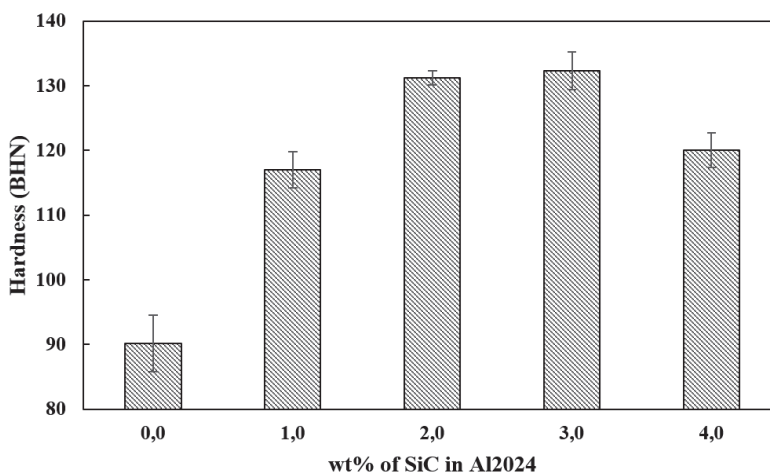


Figure 7: Hardness of Al2024-SiC composites.

### Tensile properties

Fig. 8 illustrates the tensile properties of Al2024-SiC composites, highlighting the significant improvements in tensile strength achieved with varying weight fractions of silicon carbide nanoparticles. The tensile test results for the Al-2024 alloy and 1-4% SiC nanoparticle reinforcements show significant improvements in mechanical properties. Adding SiC nanoparticles to the Al-2024 alloy increased yield strength and ultimate tensile strength (UTS) across all compositions while the percentage elongation decreased slightly. The yield strength for the base Al-2024 alloy was 125.3 MPa, and the UTS was 175.1 MPa. At 3% SiC, the yield strength peaked at 188.2 MPa, and the UTS attained its highest value of 294.9 MPa. However, with 4% SiC, the yield strength slightly decreased to 162.5 MPa, and the UTS dropped to 232.5 MPa, indicating that an optimal reinforcement level was achieved at 3% SiC. The slight reduction in percentage elongation with increasing SiC content indicates a trade-off between strength and ductility, as higher reinforcement levels generally enhance strength at the cost of reduced ductility.

The tensile testing results indicate a significant 25% improvement in strength values when SiC nanoparticles were added to the Al-2024 alloy. This highlights the effectiveness of SiC reinforcement in substantially enhancing the material's mechanical properties. The nanoparticles act as strong reinforcements, refine grains, and create obstacles for dislocation movement. Additionally, the uniform dispersion of SiC using ultrasonic-assisted casting contributes to consistent and improved strength.

### Strengthening mechanisms

The particle size and content strongly influence the strength of processed composites [21]. According to the dispersion strengthening mechanism, larger particles may cause voids to form around them, which could weaken the composite. On the other hand, using nanoparticles for reinforcement efficiently promotes particle hardening processes, increasing the matrix's mechanical strength. The impact of several strengthening mechanisms to strength improvement is analysed in this



study using concepts from micromechanics and continuum mechanics. The study also looks at how the efficiency of these strengthening mechanisms is affected by raising the proportion of nano-SiC reinforcement in the Al-2024 alloy matrix.

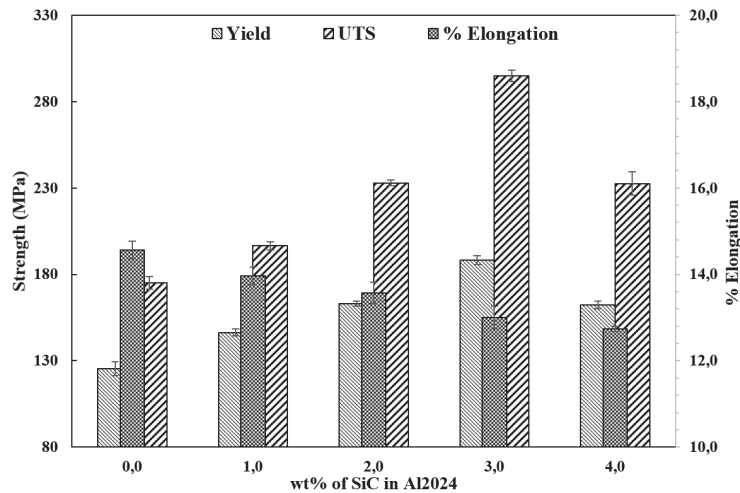


Figure 8: Tensile properties of Al2024-SiC composites.

The composite's yield strength ( $\sigma_{yc}$ ) is increased by load transfer from the soft matrix to the hard reinforcement particles, as per continuum mechanics. This can be computed as follows [22,23]:

$$\sigma_{yc} = \sigma_{ym} \left[ V_r \left( \frac{S+2}{2} \right) + V_m \right] \quad (1)$$

where  $S$  is the aspect ratio of the reinforcement particles and  $= 1$  for equiaxed particles,  $V_r$  and  $V_m$  are the reinforcement volume fractions,  $\sigma_{ym}$  is the matrix yield strength.

It is possible to quantify the Orowan strengthening contribution to the increased composite yield strength as follows [24]:

$$\Delta\sigma_{Orowan} = \frac{0.13Gb}{\lambda} \ln \frac{D}{2b} \quad (2)$$

where  $D$  is the mean particle diameter,  $b$  is the Burgers vector,  $G$  is the matrix alloy's shear modulus, and  $\lambda$  is the interparticle distance between edges, which can be written as follows:

$$\lambda = D \sqrt{\left( \frac{\pi}{6V_r} - \frac{2}{3} \right)} \quad (3)$$

For the Al2024 alloy, the Burgers vector,  $b$ , is 0.286 and the shear modulus,  $G$ , is 28 GPa. For nano-SiC reinforcement particles with an average particle size of  $D$  of 20 nm, the value of  $\lambda$  has been estimated by changing  $\lambda$ ,  $G$ ,  $b$ , and  $D$  values in Eqs. (2) and (3).

According to the Taylor strengthening mechanism, the dislocation strengthening contribution to the improvement of composite yield strength can be calculated as follows [22–24]:

$$\Delta\sigma_{CTE} = Gb\sqrt{\rho} \quad (4)$$

Here,  $\rho$  is the dislocation density caused by CTE mismatch and is given as [22], while  $\eta$  is a constant that is roughly equal to 1:

$$\rho = \frac{12\Delta\alpha\Delta TV_r}{DbV_m} \quad (5)$$

In this case,  $\Delta\alpha$  represents the CTE difference between the matrix alloy ( $23.6 \times 10^{-6} \text{ K}^{-1}$ ) and reinforcement particles ( $4.6 \times 10^{-6} \text{ K}^{-1}$ ). The difference between the test temperature ( $20^\circ\text{C}$ ) and the temperature at which the reinforcing particles are introduced ( $750^\circ\text{C}$ ) is known as  $\Delta T$ . The test temperature in this study is the mold's preheated temperature for transferring the composite slurry [25].

The Hall-Petch relationship is used to assess the increase in yield strength brought about by grain refinement:

$$\Delta\sigma_{Hall-Petch} = k \left[ d^{-\frac{1}{2}} - d_o^{-\frac{1}{2}} \right] \quad (6)$$

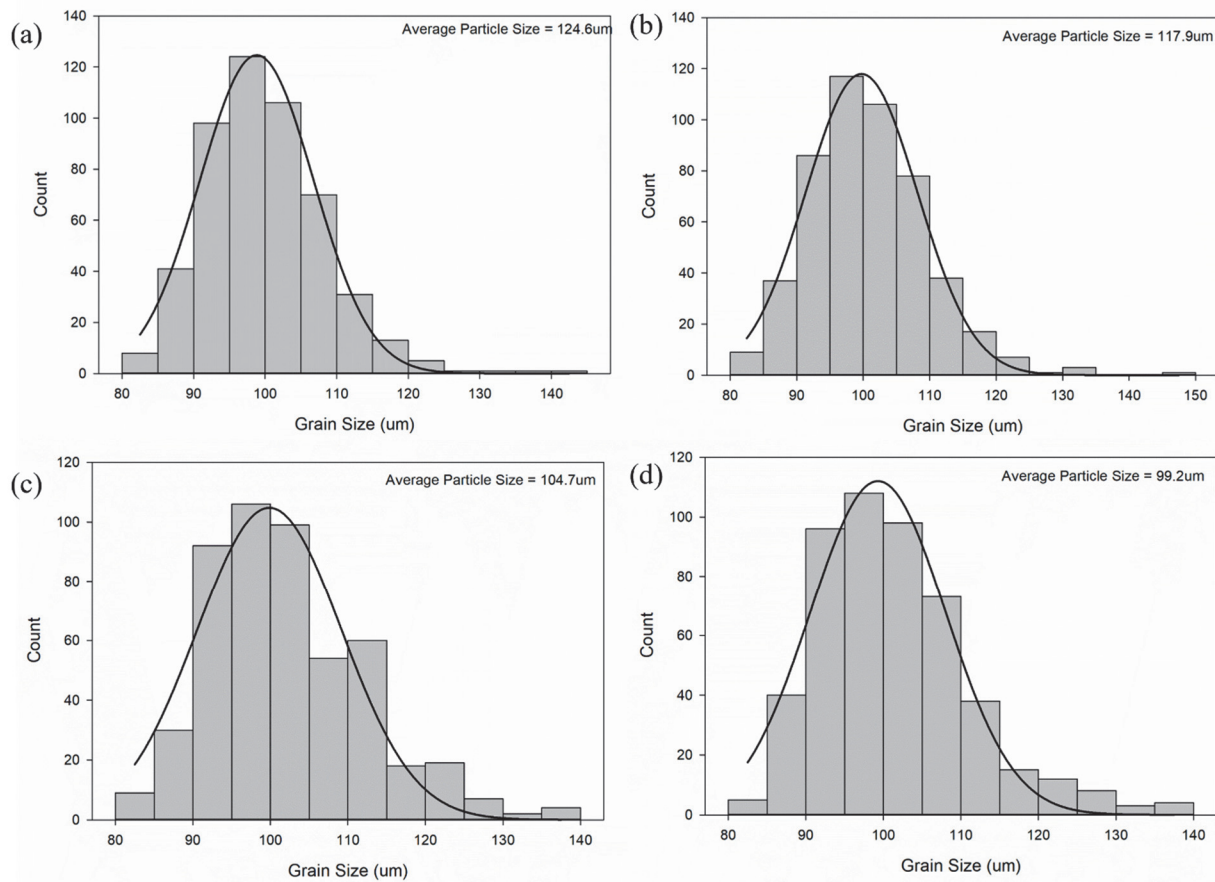


Figure 9: Grain size distribution curve of Al2024/SiC nanocomposites with (a) 1wt%, (b) 2wt%, (c) 3wt%, (d) 4wt% of SiC.

In this case,  $k$  is the matrix's Hall–Petch slope. The average grain size of the matrix alloy is  $d$ , the average size of the reinforcement particles is  $d_o=20 \text{ nm}$ , and the value of  $k$  for pure aluminium is  $\approx 74 \times 10^{-3} \text{ MPa}\sqrt{\text{m}}$ . Fig. 6 (a-d) is used to estimate the average grain size values for various reinforcing circumstances, and Fig. 9 (a-d) displays the estimated grain size ' $d$ ' distribution.

The equation for predicting the enhanced yield strength of the composites for each designated reinforcement condition is provided below [25], which is derived from a combination of the contributions of the micromechanics strengthening mechanisms previously discussed.

$$\sigma_{ym} = \sigma_{alloy} + \Delta\sigma_{Hall-Petch} + \sqrt{(\Delta\sigma_{Ornman})^2 + (\Delta\sigma_{CTE})^2} \quad (7)$$

Here,  $\sigma_{alloy}$  is the yield strength of the as-cast A2024 aluminium matrix alloy treated with ultrasonic cavitations. The experimentally measured value of  $\sigma_{alloy}$  in this investigation is 125.3 MPa.

Tab. 2 shows the estimated yield strength contribution for each strengthening process. While the contribution of strength increase owing to grain refinement is relatively modest because the Hall–Petch slope is smaller for pure aluminium, the contribution of yield strength enhancement due to thermal mismatch is more closely followed by the Orowan strengthening [24]. The findings further imply that the primary strengthening mechanism in nano-SiC particle-reinforced aluminium 2024 matrix composites manufactured using an ultrasonic cavitation-assisted stir casting technique is strengthening due to thermal dislocation.

Composite	Experimental Yield Strength (MPa)	Predicted Yield Strength (MPa)				Load Transfer Mechanism
		Orowan Mechanism	Dislocation Strengthening	Grain Refinement Strengthening	Total Yield Strength (Eqn. 7)	
Al2024+1wt%SiC	146.3	25.7	3.7	6.6	157.9	125.9
Al2024+2wt%SiC	163.0	36.6	5.3	6.8	169.1	126.6
Al2024+3wt%SiC	188.2	45.2	6.5	7.2	178.2	127.2
Al2024+4wt%SiC	162.5	52.5	7.6	7.4	185.8	127.8

Table 2: Comparison of different strengthening mechanisms to yield strength of the composite.

Compared to the theoretically expected values, the yield strength values obtained through experimentation are lower. The presence of residual nano-SiC particle clusters in the composites, along with measurement errors in particle aspect ratio and particle and grain size, may cause a decrease in yield strength values. Defects that led to the early failure were established by weaker interparticle bond strength in clusters than the binding strength between the ceramic particle and matrix.

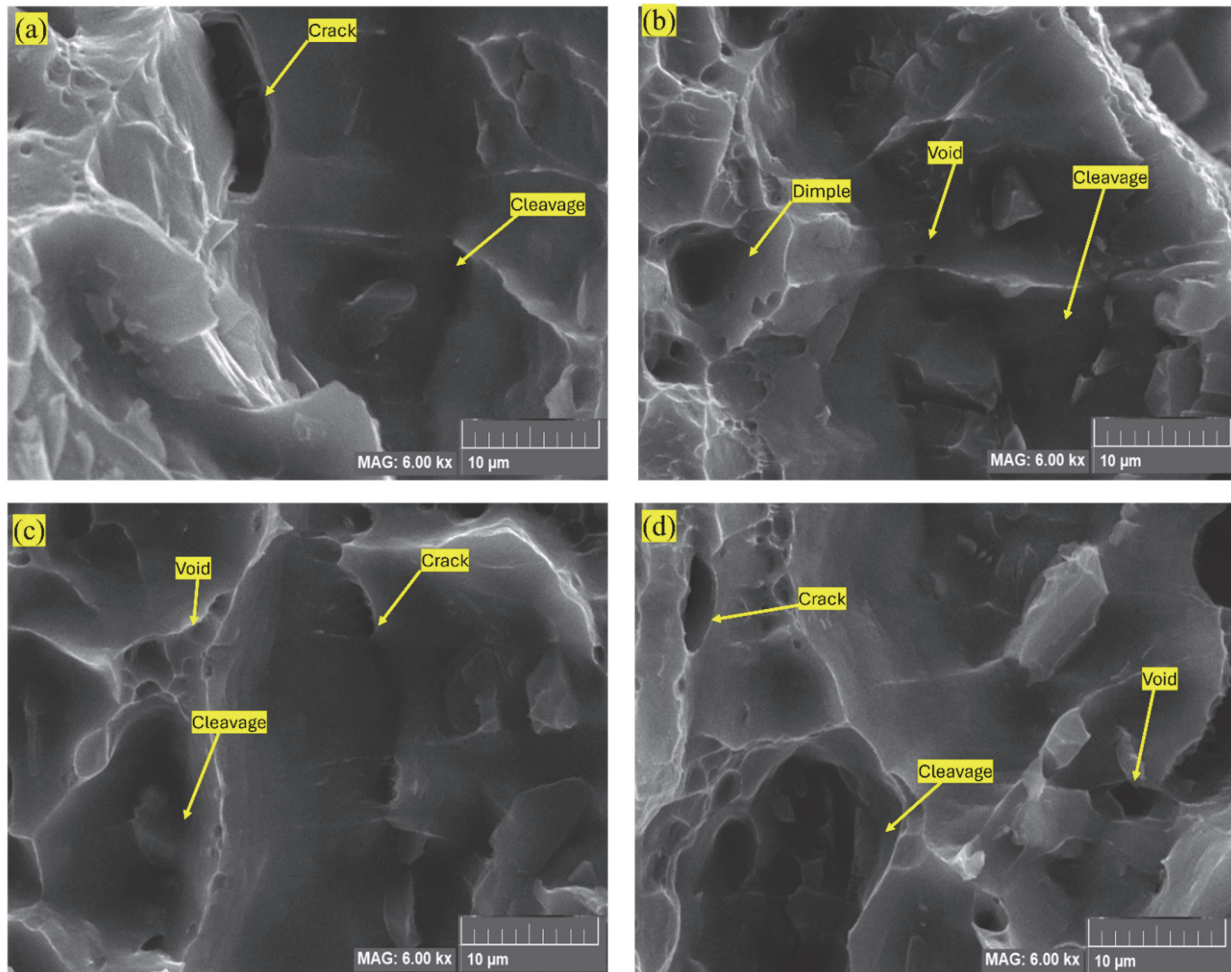


Figure 10: SEM images of the Al2024 composites with (a) 1wt%, (b) 2wt%, (c) 3wt%, (d) 4wt% of SiC.



### Fractography

The SEM, shown in Fig. 10, fractography images of the Al2024-SiCnp composite with 1 wt%, 2 wt%, 3 wt%, and 4 wt% reveal key microstructural features indicative of the composite's fracture behaviour. Across all four images, dimples are prominently observed, suggesting a ductile fracture mode in the Al-2024 matrix. These dimples indicate that the Al2024-SiCnp composite underwent localised plastic deformation, absorbing energy during fracture.

Along with dimples, voids are also visible throughout the microstructure of the Al2024-SiCnp composite. These voids likely form around the SiC nanoparticles due to localised stress concentrations, which may cause debonding between the Al-2024 and SiC nanoparticles. This debonding contributes to the initiation and growth of voids, a common feature in ductile fracture.

The SEM images also show cleavages and microcracks, which indicate that some areas have brittle fracture properties. The cleavages suggest that brittle fracture may occur in specific matrix regions, particularly in areas with high-stress concentrations or densely packed SiC particles. Particle agglomerations or stress intensities surrounding the reinforcing particles may cause these brittle characteristics, which limit plastic flow and promote crack propagation.

The mix of dimples, voids, cleavages, and cracks in these fractography images shows a mixed-mode fracture behaviour, with the SiC nanoparticle reinforcement influencing both brittle and ductile properties of the Al2024-SiCnp composite. More voids and cleavages have been formed due to higher stress concentrations of increased SiC nanoparticles, which led to more complex fracture behaviour; however, the composite's strength and hardness were improved.

Ultrasonic-assisted stir casting enhances particle-matrix bonding, improving hardness in Al2024-SiCnp composites. However, at 4% SiC, nanoparticle clustering reduces reinforcement effectiveness. Fractography analysis shows mixed-mode fracture behavior, with dimples indicating ductile fracture and cleavages suggesting localized brittleness due to higher stress concentrations.

## CONCLUSIONS

The mechanical characteristics of the Al2024-SiCnp composite have been investigated in this work, focusing on the function of ultrasonic-assisted stir casting in attaining uniform distribution of reinforcement. The experimental findings confirm SiC nanoparticles' promise for various engineering applications and offer detailed information on enhanced mechanical performance. The following are the conclusions drawn from the study:

- Applying ultrasonic-assisted stir casting was pivotal in achieving a uniform distribution of SiC nanoparticles within the Al-2024 matrix, which enhanced the interaction between the matrix and reinforcement, thereby optimising the overall mechanical properties of the Al2024-SiCnp composite.
- According to the experimental results of hardness tests, adding SiC nanoparticles significantly increased hardness values by 31%. Tensile strength tests, in contrast, showed a significant 25% increase in strength, demonstrating how well nanoparticle reinforcement works to improve material qualities.
- The study identified several strengthening mechanisms contributing to yield strength, including the Orowan mechanism, dislocation strengthening, and grain refinement strengthening. A comparison between the experimental and predicted yield strength of the Al2024-SiCnp composite revealed a maximum variation of 13%, indicating a close alignment between the theoretical predictions and actual performance. This demonstrates the reliability of the predictive models used in this research for assessing the mechanical behaviour of the composite.

This composite improves resilience in military vehicles and armour in defence applications, while its lightweight properties benefit sporting goods like bicycle frames. Its corrosion resistance makes it suitable for marine applications, including ship structures.

Future research should analyse a broader range of mechanical properties, such as fatigue and impact resistance. Long-term durability studies and multiscale modelling will enhance performance predictions, while application-specific tailoring will optimise properties for targeted uses and address sustainability concerns.

## FUNDING

This research received no specific grant from any funding agency in the public, commercial, or not-for-profit sectors.



## CONFLICT OF INTEREST

The authors declare that they have no conflict of interest.

## REFERENCES

- [1] Ovalı, İ., Esen, C., Albayrak, S., Karakoç, H., Saravana, K.M., Che, H.Y. (2023). Mechanical Properties of Al<sub>2</sub>O<sub>3</sub>/Al<sub>2</sub>O<sub>3</sub>/MgO/Graphite composites via hydro-thermal hot pressing route, *Mater. Chem. Phys.*, 302(127779), DOI: 10.1016/j.matchemphys.2023.127779.
- [2] Karabacak, A.H., Çanakçı, A., Çelebi, M., Güler, O., Tunç, S.A., Arpacı, K.A. (2023). Production of Al<sub>2</sub>O<sub>3</sub>/h-BN nanocomposites with improved corrosion, wear and mechanical properties, *Mater. Chem. Phys.*, 300(127566), DOI: 10.1016/j.matchemphys.2023.127566.
- [3] Siguerdjidjene, H., Houari, A., Madani, K., Amroune, S., Mokhtari, M., Mohamad, B., Campilho, R. (2024). Predicting Damage in Notched Functionally Graded Materials Plates through extended Finite Element Method based on computational simulations, *Frat. Ed Integrità Strutt.*, 18(70), pp. 1–23, DOI: 10.3221/IGF-ESIS.70.01.
- [4] Lingaraju, S.V., Mallikarjuna, C., Doddamani, S. (2023). Effect of addition of TiC nanoparticles on the tensile strength of Al<sub>7075</sub>-graphene hybrid composites, *Res. Eng. Struct. Mater.*, 9(1), pp. 19–30, DOI:10.17515/resm2022.486ma0725.
- [5] Lingaraju, S.V., Mallikarjuna, C., Venkatesha, B.K. (2022). Investigation on Wear Analysis of Aluminium (Al) 7075 Alloy Reinforced with Titanium Carbide (TiC) and Graphene (Gr) Nanoparticles, *Solid State Phenom.*, 339, pp. 125–134, DOI: 10.4028/p-2j6mh8.
- [6] Lingaraju, S.V., Jadhav, M.R., Doddamani, S., Hatti, G., Dhuttargaon, M.S. (2024). Investigation on Tribological Behavior of Al<sub>7075</sub>-TiC/Graphene Nano-composite Using Taguchi Method, *J Bio Tribo Corros*, 10(110), DOI: 10.1007/s40735-024-00908-3.
- [7] Ramesh, R.S., Santhosh Kumar, M.V., Yasmin B., Doddamani, S., Kaleemulla, M.K. (2023). Fracture toughness investigations of AA6061-SiC composites : Effect of corrosion parameters, *Mater. Chem. Phys.*, 308, pp. 128224, DOI: 10.1016/j.matchemphys.2023.128224.
- [8] Doddamani, S., Kaleemulla, M.K. (2017). Experimental investigation on fracture toughness of Al<sub>6061</sub>–graphite by using Circumferential Notched Tensile Specimens, *Frat. Ed Integrità Strutt.*, 11(39), pp. 274–281, DOI: 10.3221/IGF-ESIS.39.25.
- [9] Yasmin, B., Bharath, K.N., Doddamani, S., Rajesh A.M., Kaleemulla, M.K. (2020). Optimization of Process Parameters of Fracture Toughness Using Simulation Technique Considering Aluminum–Graphite Composites, *Trans. Indian Inst. Met.*, 73(12), pp. 3095–3103, DOI: 10.1007/s12666-020-02113-5.
- [10] Bharath, K.N., Doddamani, S., Rajesh A.M., Kaleemulla, M.K. (2023). Simulation of Various Fracture Models by Varying Geometrical Parameters using Taguchi’s DOE, *Struct. Integr. Life*, 23(2), pp. 191–195.
- [11] Rajesh A.M., Bharath, K.N., Doddamani, S., Kaleemulla, M.K. (2019). Material characterization of SiC and Al<sub>2</sub>O<sub>3</sub> reinforced hybrid aluminum metal matrix composites on wear behavior, *Adv. Compos. Lett.*, 28(1–10), DOI: 10.1177/0963693519856356.
- [12] Rajesh A.M., Bharath, K.N., Doddamani, S., Kaleemulla, M.K. (2019). Generation of mechanically mixed layer during wear in hybrid aluminum MMC under as - cast and age hardened conditions, *SN Appl. Sci.*, 1(860), DOI: 10.1007/s42452-019-0906-5.
- [13] Hareesha G., Chikkanna N., Doddamani, S. (2021). Taguchi’s method of optimization of fracture toughness parameters of Al-SiCp composite using compact tension specimens, 11(2), pp. 152-157.
- [14] Reddy, A.P., Krishna, P.V., Rao, N.R. (2018). Mechanical and wear properties of aluminium based nanocomposite fabricated through ultrasonic assisted stir casting, *J. Test. Eval.*, 48, pp. 22–43, DOI: 10.1520/JTE20170560.
- [15] Singh, V, Murtaza, Q., Niranjana, M.S. (2024). Analyzing the synergistic effects of hard ceramic TiB<sub>2</sub> and rare earth oxide La<sub>2</sub>O<sub>3</sub> on mechanical behaviour, wear resistance, and residual stress of AA6061-T6 hybrid composite fabricated via ultrasonic-assisted stir casting, *Mater. Chem. Phys.*, 325(129727), DOI: 10.1016/j.matchemphys.2024.129727.
- [16] Gupta, R.K, Ravi, K.R., Udhayabanu, V., Peshwe, D.R. (2022). Effect of ultrasonic treatment on microstructural and mechanical properties of Al 7075/Grp composite, *Mater. Chem. Phys.*, 281(125905), DOI: 10.1016/j.matchemphys.2022.125905.



- [17] Rao, T.B. (2021). Microstructural, mechanical, and wear properties characterization and strengthening mechanisms of Al7075/SiCnp composites processed through ultrasonic cavitation assisted stir-casting, *Mater. Sci. Eng. A*, 805(140553), DOI: 10.1016/j.msea.2020.140553.
- [18] Venkatesh, V.S.S., Rao, G. P., Patnaik, L., Gupta, N., Kumar, S., Saxena, K.K., Sunil, B.D.Y. Eldin, S.M. and Al-kafaji, F.H.M. (2023). Processing and evaluation of nano SiC reinforced aluminium composite synthesized through ultrasonically assisted stir casting process, *J. Mater. Res. Technol.*, 24, pp. 7394–7408, DOI: 10.1016/j.jmrt.2023.05.030.
- [19] Alqahtani, I., Niyaz Ahamed, M.B., Ashoka, E., Rajesh, A.M., Bharath, P.B., Doddamani, S. (2025). Indentation Fracture Toughness of Aluminium-Graphite Composites: Influence of Nano-particles, *Frat. Ed Integrità Strutt.*, 19(71), pp. 11–21, DOI: 10.3221/IGF-ESIS.71.02.
- [20] Aldriasawi S.K., Ameen, N.H., Fadheel, K.I., Anead, A.M., Mhabes, H.E., Mohamad, B.A. (2024). An Experimental Artificial Neural Network Model: Investigating and Predicting Effects of Quenching Process on Residual Stresses of AISI 1035 Steel Alloy, *J. Harbin Inst. Technol. Ser.*, 31(5), pp. 78–92, Doi: DOI:10.11916/j.issn.1005-9113.2023090.
- [21] Makri, H., Saib, C., Amroune, S., Zergane, S., Mohamad, B., Benarioua, M., Necib, K. (2024). Elaboration and characterization of Cu–Zn–Al shape memory alloys, *Pollack Period.*, , DOI: 10.1556/606.2024.01122.
- [22] Jayalakshmi, S., Gupta, S., Sankaranarayanan, S., Sahu, S., Gupta, M. (2013). Structural and mechanical properties of Ni60Nb40 amorphous alloy particle reinforced Al-based composites produced by microwave-assisted rapid sintering, *Mater. Sci. Eng., A*, 581, pp. 119–127.
- [23] Zhang, Q., Xiao, B.L., Wang, W.G., Ma, Z.Y. (2012). Reactive mechanism and mechanical properties of in situ composites fabricated from an Al-TiO<sub>2</sub> system by friction stir processing, *Acta Mater*, 60(20), pp. 7090–7103.
- [24] Gupta, R., Chaudhari, G.P., Daniel, B.S.S. (2018). Strengthening mechanisms in ultrasonically processed aluminium matrix composite with in-situ Al<sub>3</sub>Ti by salt addition, *Compos. B Eng.*, 140, pp. 27–34.
- [25] Chen, F., Chen, Z., Mao, F., Wang, Tongmin., Cao, Z. (2015). TiB<sub>2</sub> reinforced aluminum based in situ composites fabricated by stir casting, *Mater. Sci. Eng., A*, 625, pp. 357–368.